

Uplink Analysis of Large MU-MIMO Systems With Space-Constrained Arrays in Ricean Fading

Harsh Tataria*, Peter J. Smith[†], Michail Matthaiou[‡], and Pawel A. Dmochowski*

* School of Engineering and Computer Science, Victoria University of Wellington, Wellington, New Zealand

[†] School of Mathematics and Statistics, Victoria University of Wellington, Wellington, New Zealand

[‡] School of Electronics, Electrical Engineering and Computer Science, Queen's University Belfast, Belfast, Northern Ireland, UK
email: {harsh.tataria, pawel.dmochowski}@ecs.vuw.ac.nz, peter.smith@vuw.ac.nz, m.matthaiou@qub.ac.uk

Abstract—Closed-form approximations to the expected per-terminal signal-to-interference-plus-noise-ratio (SINR) and ergodic sum spectral efficiency of a large multiuser multiple-input multiple-output system are presented. Our analysis assumes correlated Ricean fading with maximum ratio combining on the uplink, where the base station (BS) is equipped with a uniform linear array (ULA) with physical size restrictions. Unlike previous studies, our model caters for the presence of unequal correlation matrices and unequal Rice factors for each terminal. As the number of BS antennas grows without bound, with a finite number of terminals, we derive the limiting expected per-terminal SINR and ergodic sum spectral efficiency of the system. Our findings suggest that with restrictions on the size of the ULA, the expected SINR saturates with increasing operating signal-to-noise-ratio (SNR) and BS antennas. Whilst unequal correlation matrices result in higher performance, the presence of strong line-of-sight (LoS) has an opposite effect. Our analysis accommodates changes in system dimensions, SNR, LoS levels, spatial correlation levels and variations in fixed physical spacings of the BS array.

I. INTRODUCTION

The deployment of large numbers of antennas at a cellular base station (BS) to communicate with multiple user terminals has received a considerable amount of attention recently [1, 2]. Specifically, large (a.k.a. massive) multiuser multiple-input multiple-output (MU-MIMO) systems have been shown to achieve orders of magnitude greater performance than conventional MU-MIMO systems, due to their ability to leverage favorable propagation conditions [2]. Nevertheless, the emergence of such systems has posed new engineering challenges which must be overcome before their adoption on a scale commensurate with their true potential. One of the critical issues is accommodating large numbers of antennas in fixed physical spacings [3, 4]. This tends to increase the level of spatial correlation and antenna coupling, as successive elements are placed in close proximity with inter-element spacings less than the desired half-a-wavelength [3]. This is known to cause a detrimental impact on the terminal signal-to-interference-plus-noise-ratio (SINR) and system spectral efficiency. It is thus important to rigorously analyze and evaluate the performance of systems with space-constrained (SC) antenna arrays.

Numerous works have investigated the impact of SC antenna arrays on the performance of large MU-MIMO systems (see e.g., [3–9] and references therein). Specifically, [3] analyzed the ergodic sum spectral efficiency of large MU-MIMO systems with fixed array dimensions. The authors in [4]

demonstrated that multiuser interference does not vanish in SC MU-MIMO systems with growing numbers of antennas. The uplink performance with maximum-ratio combining (MRC), zero-forcing and minimum-mean-squared-error receivers has been analyzed in [5, 7] where the authors derive upper and lower bounds on the ergodic sum spectral efficiency. Moreover, [6, 8, 9] investigated the energy efficiency performance of SC systems with various large-scale antenna array topologies considering antenna coupling.

However, very few of the above mentioned studies¹ consider the effects of line-of-sight (LoS) components, which may be a dominant feature in future wireless access with the use of smaller cell sizes, potentially operating in the millimeter-wave (mmWave) frequency bands [11–13]. Hence, understanding the performance of SC systems with LoS presence, i.e., with Ricean fading is of particular importance. Moreover, the respective channel models in [5, 7, 9] assume that all terminals are seen by the BS array via the same set of incident directions, resulting in common (equal) spatial correlation structures. In reality, differences in the local scattering around the physical location of each terminal gives rise to wide variations in the correlation patterns [14]. In addition to the small inter-element spacings, this further contributes to the level of correlation in the channel, impacting the terminal SINR and system spectral efficiency. Thus, to more accurately capture the correlation differences in multiple channels, we consider distinct correlation matrices for each terminal. Motivated by the aforementioned considerations, with a SC uniform linear array (ULA), we present a framework for analyzing the expected per-terminal SINR and ergodic sum spectral efficiency of large MU-MIMO systems with MRC at the BS. Specifically, our main contributions are as follows:

- We analyze the performance of MU-MIMO systems with SC ULAs under correlated Ricean fading channels. In doing so, we extend and generalize the SC channel models presented in [3–9] to cater for unequal correlation matrices and unequal Rice factors for each terminal. To the best of the authors' knowledge, such generality in the channel model has not previously been considered.

¹We make an exception in [4], which considers pure LoS channels. This is an extreme case, which in general may not be realizable in practice, even at mmWave frequencies, where on average 1–3 scattering clusters are anticipated in the propagation channel (see e.g., [10]).

- With MRC at the BS, we derive tight closed-form approximations to the expected per-terminal SINR and ergodic sum spectral efficiency. We show that a SC antenna deployment causes a saturation of the expected SINR with increasing numbers of BS antennas and operating signal-to-noise-ratios (SNRs).
- With a fixed number of terminals, as the number of BS antennas increases without bound, we derive novel limiting expected SINR and ergodic spectral efficiency expressions to demonstrate the convergence behavior of large SC MU-MIMO systems.
- Finally, we present special cases of the derived analytical results when NLoS components are present with equal and unequal correlation matrices, as well as, when each terminal having LoS has fixed correlation matrices.

Notation. Boldface upper and lower case symbols denote matrices and vectors, respectively. Moreover, \mathbf{I}_M denotes the $M \times M$ identity matrix. $(\cdot)^T$, $(\cdot)^H$ and $(\cdot)^{-1}$ denote the transpose, Hermitian transpose and inverse operators, respectively. We use $[\mathbf{H}]_{i,j}$ to refer to the (i,j) -th element of \mathbf{H} , whilst $\mathbf{h} \sim \mathcal{CN}(\mu, \sigma^2)$ denotes a complex Gaussian distribution for \mathbf{h} , where each element of \mathbf{h} has a mean μ and variance σ^2 . We use $x \sim u[a, b]$ to denote a uniform random variable for x taking on values from a to b . $\|\cdot\|$, $\|\cdot\|_F$ and $|\cdot|$ denote the standard two norm, Frobenius norm and scalar norm, respectively. Finally, $\text{tr}[\cdot]$ and $\mathbb{E}[\cdot]$ denote the trace and statistical expectation operations.

II. SYSTEM MODEL

We consider the uplink of a large MU-MIMO system operating in an urban microcellular (UMi) environment, where L non-cooperative single-antenna user terminals transmit data to M receive antennas at the BS ($M \gg L$) in the same time-frequency interval. The BS comprises of a ULA with equispaced, omnidirectional antennas. We assume channel knowledge at the BS with narrow-band transmission and no uplink power control. The composite $M \times 1$ received signal at the BS array can be written as

$$\mathbf{y} = \rho^{\frac{1}{2}} \mathbf{G} \mathbf{D}^{\frac{1}{2}} \mathbf{s} + \mathbf{n}, \quad (1)$$

where ρ is the average transmit power of each terminal, \mathbf{G} denotes the $M \times L$ fast-fading uplink channel matrix between M BS antennas and L terminals (discussed further in Section II-A), \mathbf{D} is an $L \times L$ diagonal matrix of link gains for the L terminals in the system, such that $[\mathbf{D}]_{l,l} = \beta_l$. The large-scale fading effects for terminal l are captured in $\beta_l = \varrho \zeta_l (r_0/r_l)^\alpha$. In particular, ϱ denotes the unit-less constant for geometric attenuation at a reference distance r_0 , r_l denotes the link distance between the BS array and terminal l , α denotes the attenuation exponent and ζ_l models the effects of shadow-fading following a log-normal density, i.e., $10 \log_{10}(\zeta_l) \sim \mathcal{N}(0, \sigma_{\text{sh}}^2)$, with σ_{sh} denoting the shadow-fading standard deviation. Numerical values for the above are tabulated in Section VI. The $L \times 1$ vector of uplink data symbols from the L terminals is given by \mathbf{s} , such that the l -th entry of \mathbf{s} , s_l has $\mathbb{E}[|s_l|^2] = 1$. Additive white Gaussian noise entries at the M BS antennas is given by the $M \times 1$

vector \mathbf{n} , such that the l -th entry of \mathbf{n} , $n_l \sim \mathcal{CN}(0, \sigma^2)$. We assume that $\sigma^2 = 1$, hence the average uplink SNR, defined as $\rho/\sigma^2 = \rho$.

A. Channel Model

Previous studies (e.g., [5, 7, 9]) on large SC MU-MIMO systems consider a physical channel model based on full NLoS propagation conditions, where the BS sees the same set of scattered directions from each terminal. We extend this model to cater for the presence of LoS in the propagation channel, as well as a unique set of scattered directions from each terminal taking into account differences in the local scattering around each terminal. Specifically, $\mathbf{G} = [\mathbf{g}_1, \dots, \mathbf{g}_L]$, where \mathbf{g}_l , the l -th column of \mathbf{G} contains the $M \times 1$ uplink channel vector from terminal l to the BS array given by

$$\mathbf{g}_l = \eta'_l \mathbf{A}_l \mathbf{h}_l + \bar{\eta}_l \bar{\mathbf{h}}_l, \quad (2)$$

where $\eta'_l = \eta_l \frac{1}{\sqrt{P}}$ with $\eta_l = (\frac{1}{1+K_l})^{\frac{1}{2}}$ and $\bar{\eta}_l = (\frac{K_l}{K_l+1})^{\frac{1}{2}}$. In the above, η_l and $\bar{\eta}_l$ balance the amount of power present in the diffuse and specular components of the channel according to the Ricean K -factor, K_l , specific to terminal l [15]. Moreover, η_l is further scaled by a factor of $\frac{1}{\sqrt{P}}$ to normalize the steering vectors in \mathbf{A}_l , the $M \times P$ receive steering matrix associated with the diffuse components of the channel. Here, P denotes a large yet finite number of diffuse wavefronts. For ULAs

$$\mathbf{A}_l = [\mathbf{a}(\phi_{l,1}), \mathbf{a}(\phi_{l,2}), \dots, \mathbf{a}(\phi_{l,P})], \quad (3)$$

where each vector in (3) is given by

$$\mathbf{a}(\phi_{l,i}) = [1, e^{j2\pi d \sin(\phi_{l,i})}, \dots, e^{j2\pi(M-1)d \sin(\phi_{l,i})}]. \quad (4)$$

We note that $i \in \{1, \dots, P\}$, with d denoting the equidistant inter-element spacing normalized by the carrier wavelength, λ ; $\phi_{l,i} \in [-\Delta/2, \Delta/2]$ denotes the i -th direction-of-arrival (DOA) from terminal l to the BS array and Δ is the angular spread in the azimuth domain. With such a model, the angular spread can be modeled by having a large P , whilst different degrees of receive correlation are adjusted by varying the angular spread. Moreover, $\mathbf{h}_l \sim \mathcal{CN}(0, \mathbf{I}_P)$ is the $P \times 1$ vector of diffuse channel gains, whilst $\bar{\mathbf{h}}_l$ is the $M \times 1$ vector denoting the specular component of the channel and is governed by the ULA's steering response with a LoS DoA, $\bar{\phi}_l$ for terminal l , such that

$$\bar{\mathbf{h}}_l = [1, e^{j2\pi d \sin(\bar{\phi}_l)}, \dots, e^{j2\pi(M-1)d \sin(\bar{\phi}_l)}]. \quad (5)$$

Remark 1. For both $\mathbf{a}(\phi_{l,i})$ and $\bar{\mathbf{h}}_l$, we note that the normalized total array length, d_0 , is fixed at the BS, such that the inter-element spacing between two successive elements is given by $d = \frac{d_0}{M-1} \lambda$. Since the physical dimensions of the BS array are predetermined, the above model accurately allows us to capture the correlation due to close proximity of adjacent antenna elements positioned at the array. This along with the unique correlation matrices for each terminal created by the \mathbf{A}_l for $l \in \{1, \dots, L\}$ constitutes our focus in the following sections. We note that in this study, we neglect the effects of antenna coupling, since they can be compensated by impedance matching techniques as shown in [6, 16].

To determine the level of LoS and NLoS present in the propagation channel from a given terminal to the BS, we

employ a probability based approach following [12]. Both LoS and NLoS probabilities are a function of the link distance, from which the LoS and NLoS geometric attenuation, as well as other link characteristics are obtained. We consider propagation parameters from both microwave [17] and mmWave [10] frequency bands. For notational clarity, we delay the discussion of the above mentioned parameters to Section VI.

B. Per-Terminal SINR and Ergodic Sum Spectral Efficiency

As linear signal processing techniques perform near optimally for large MU-MIMO systems [1, 2], we employ a linear receiver in the form of a MRC at the BS. The $L \times M$ MRC matrix, \mathbf{G}^H , is used to separate \mathbf{y} into L streams by

$$\mathbf{r} = \mathbf{G}^H \mathbf{y} = \rho^{\frac{1}{2}} \mathbf{G}^H \mathbf{G} \mathbf{D}^{\frac{1}{2}} \mathbf{s} + \mathbf{G}^H \mathbf{n}. \quad (6)$$

Thus, the detected signal from terminal l is given by

$$r_l = \rho^{\frac{1}{2}} \beta_l^{\frac{1}{2}} \mathbf{g}_l^H \mathbf{g}_l s_l + \rho^{\frac{1}{2}} \sum_{k=1, k \neq l}^L \beta_k^{\frac{1}{2}} \mathbf{g}_l^H \mathbf{g}_k s_k + \mathbf{g}_l^H \mathbf{n}, \quad (7)$$

resulting in the corresponding SINR given by

$$\text{SINR}_l = \frac{\rho \beta_l \|\mathbf{g}_l\|^4}{\|\mathbf{g}_l\|^2 + \rho \sum_{k=1, k \neq l}^L \beta_k \|\mathbf{g}_l\| \|\mathbf{g}_k\|^2}. \quad (8)$$

Hence, the instantaneous achievable uplink spectral efficiency for terminal l (measured in bits/sec/Hz) can be computed as $R_l = \log_2(1 + \text{SINR}_l)$. As such, the ergodic sum spectral efficiency over all L terminals is given by

$$\mathbb{E}[\mathbf{R}_{\text{sum}}] = \mathbb{E} \left[\sum_{l=1}^L R_l \right], \quad (9)$$

where the expectation is performed over the fast-fading. In the following section, we derive tight analytical expressions to approximate the expected value of (8) and (9), respectively.

III. EXPECTED PER-TERMINAL SINR AND ERGODIC SUM SPECTRAL EFFICIENCY ANALYSIS

The expected SINR for terminal l can be obtained by taking the expectation of the ratio in (8). However, exact evaluation of this is extremely cumbersome [18, 19]. Hence, we resort to the commonly used first-order Delta expansion, as shown in [18, 19] and references therein. This gives

$$\mathbb{E}[\text{SINR}_l] \approx \frac{\rho \beta_l \mathbb{E}[\|\mathbf{g}_l\|^4]}{\mathbb{E}[\|\mathbf{g}_l\|^2] + \rho \sum_{k=1, k \neq l}^L \beta_k \mathbb{E}[\|\mathbf{g}_l\| \|\mathbf{g}_k\|^2]}. \quad (10)$$

Remark 2. The approximation in (10) is of the form of $\mathbb{E} \left[\frac{X}{Y} \right] \approx \frac{\mathbb{E}[X]}{\mathbb{E}[Y]}$. The accuracy of such approximations relies on Y having a small variance relative to its mean. This can be seen by applying a multivariate Taylor series expansion of $\frac{X}{Y}$ around $\frac{\mathbb{E}[X]}{\mathbb{E}[Y]}$, as shown in the analysis methodology of [18]. In particular, both X and Y are well suited to this approximation as M and L start to increase (the case for large MU-MIMO systems), where the approximation is shown to be extremely tight. This is due to X and Y averaging their respective individual components, minimizing their variance relative to their mean. For further discussion, we refer the interested

reader to Appendix I of [18], where a detailed mathematical proof of the approximation accuracy can be found.

In the sequel, Lemmas 1, 2 and 3 derive the expectations in the numerator and denominator of (10).

Lemma 1. For a ULA with M antennas in a fixed physical space at the BS, considering a correlated Ricean fading channel in \mathbf{g}_l from terminal l to the BS

$$\delta_l = \mathbb{E}[\|\mathbf{g}_l\|^4] = (\eta'_l)^4 \left\{ P^2 M^2 + \text{tr} \left[(\mathbf{A}_l^H \mathbf{A}_l)^2 \right] \right\} + 2PM^2(\eta'_l)^2(\bar{\eta}_l)^2 + 2(\eta'_l)^2(\bar{\eta}_l)^2 \bar{\mathbf{h}}_l^H \mathbf{A}_l \mathbf{A}_l^H \bar{\mathbf{h}}_l + (\bar{\eta}_l)^4 M^2, \quad (11)$$

where each parameter is defined after (2).

Proof: See Appendix A. ■

Lemma 2. Under the same conditions as Lemma 1,

$$\varphi_{l,k} = \mathbb{E}[\|\mathbf{g}_l\| \|\mathbf{g}_k\|^2] = (\eta'_l)^2 (\eta'_k)^2 \text{tr}[\mathbf{A}_k \mathbf{A}_k^H \mathbf{A}_l \mathbf{A}_l^H] + (\eta'_l)^2 (\bar{\eta}_k)^2 \text{tr}[\bar{\mathbf{h}}_k^H \mathbf{A}_k \mathbf{A}_l^H \bar{\mathbf{h}}_l] + (\bar{\eta}_l)^2 (\eta'_k)^2 \text{tr}[\bar{\mathbf{h}}_l^H \mathbf{A}_k \mathbf{A}_k^H \bar{\mathbf{h}}_l] + (\bar{\eta}_l)^2 (\bar{\eta}_k)^2 \bar{\mathbf{h}}_l^H \bar{\mathbf{h}}_k \bar{\mathbf{h}}_k^H \bar{\mathbf{h}}_l. \quad (12)$$

Proof: See Appendix B. ■

Lemma 3. Under the same conditions as Lemma 1,

$$\chi_l = \mathbb{E}[\|\mathbf{g}_l\|^2] = M \left[P(\eta'_l)^2 + (\bar{\eta}_l)^2 \right]. \quad (13)$$

Proof: We begin by substituting the definition of \mathbf{g}_l into χ_l and expanding, allowing us to write

$$\chi_l = \mathbb{E}[\|\mathbf{g}_l\|^2] = \mathbb{E}[(\eta'_l)^2 \mathbf{h}_l^H \mathbf{A}_l^H \mathbf{A}_l \mathbf{h}_l] + \mathbb{E}[(\bar{\eta}_l)^2 \bar{\mathbf{h}}_l^H \bar{\mathbf{h}}_l]. \quad (14)$$

Performing the expectations with respect to \mathbf{h}_l and extracting the relevant constants yields

$$\chi_l = \mathbb{E}[\|\mathbf{g}_l\|^2] = (\eta'_l)^2 \text{tr}[\mathbf{A}_l^H \mathbf{A}_l] + (\bar{\eta}_l)^2 \mathbb{E}[\bar{\mathbf{h}}_l^H \bar{\mathbf{h}}_l]. \quad (15)$$

Recognizing that $\text{tr}[\mathbf{A}_l^H \mathbf{A}_l] = PM$ and $\mathbb{E}[\bar{\mathbf{h}}_l^H \bar{\mathbf{h}}_l] = M$ allows us to state

$$\chi_l = \mathbb{E}[\|\mathbf{g}_l\|^2] = M \left[P(\eta'_l)^2 + (\bar{\eta}_l)^2 \right], \quad (16)$$

concluding the proof. ■

Theorem 1. With MRC at the BS consisting of a space-constrained ULA, the expected uplink SINR of terminal l in a spatially correlated Ricean fading channel can be approximated as

$$\mathbb{E}[\text{SINR}_l] \approx \frac{\rho \beta_l \delta_l}{\chi_l + \rho \sum_{k=1, k \neq l}^L \beta_k \varphi_{l,k}}. \quad (17)$$

Proof: Substituting the results from Lemmas 1, 2 and 3 for δ_l , $\varphi_{l,k}$ and χ_l yields the desired expression in (17). ■

Remark 3. The result in (17) is extremely general and is a closed-form solution to a complex scenario, where in addition to fixed physical spacing and MRC at the BS, each terminal has a unique LoS direction, unique Rice factor, unique receive correlation matrix and a unique link gain. It can be readily observed via inspection, that both the numerator and the denominator of (17) are influenced by each of the above factors. The result allows for a general evaluation of large MU-MIMO systems with space-constrained ULAs and lends itself to many useful special cases (as shown in Section IV).

We note that (17) can be further used to approximate the ergodic sum spectral efficiency of the system by

$$\mathbb{E}[\mathbf{R}_{\text{sum}}] \approx \sum_{l=1}^L \log_2(1 + \mathbb{E}[\text{SINR}_l]). \quad (18)$$

The accuracy of the derived closed-form expressions in (17) and (18) is demonstrated in Section VI. In the following section, we present three special cases of Theorem 1 demonstrating its generality.

IV. SPECIAL CASES

Corollary 1. With MRC at the BS consisting of a SC ULA, the expected uplink SINR of terminal l with no LoS, i.e., Rayleigh fading with unequal correlation matrices for each terminal, can be approximated as

$$\mathbb{E}[\text{SINR}_l^{C1}] \approx \frac{\rho \beta_l (\eta'_l)^4 \left\{ P^2 M^2 + \text{tr} \left[(\mathbf{A}_l^H \mathbf{A}_l)^2 \right] \right\}}{MP(\eta'_l)^2 + \rho \sum_{k=1, k \neq l}^L \left\{ \beta_k (\eta'_l)^2 (\eta'_k)^2 \text{tr} [\mathbf{A}_k \mathbf{A}_k^H \mathbf{A}_l \mathbf{A}_l^H] \right\}}. \quad (19)$$

Proof: Substituting δ_l , χ_l and φ_l into (17) and setting $\bar{\eta}_l = \bar{\eta}_k = 0$, $\eta'_l = \eta'_k = \frac{1}{\sqrt{P}}$ as $K_l = 0$ and $\bar{\mathbf{h}}_l = \bar{\mathbf{h}}_k = \mathbf{0}_{M \times 1}$, where $\mathbf{0}_{M \times 1}$ denotes a $M \times 1$ vector of zeros for $l, k \in \{1, \dots, L\}$ yielding the desired expression. ■

Corollary 2 (Proposition 1 in [7]). With MRC processing at the BS containing of a SC ULA, the expected uplink SINR for terminal l with no LoS and equal correlation matrices, i.e., Rayleigh fading with a fixed correlation for each terminal, can be approximated as

$$\mathbb{E}[\text{SINR}_l^{C2}] \approx \frac{\rho \beta_l (\eta'_l)^4 \left\{ P^2 M^2 + \text{tr} \left[(\mathbf{A}_l^H \mathbf{A}_l)^2 \right] \right\}}{MP(\eta'_l)^2 + \rho \sum_{k=1, k \neq l}^L \left\{ \beta_k (\eta'_l)^2 (\eta'_k)^2 \text{tr} \left[(\mathbf{A}_l^H \mathbf{A}_l)^2 \right] \right\}}. \quad (20)$$

Proof: Following the approach outlined in the proof of Corollary 1 and recognizing that $\text{tr}[(\mathbf{A}_l \mathbf{A}_l^H)^2] = \text{tr}[\mathbf{A}_l \mathbf{A}_l^H \mathbf{A}_l \mathbf{A}_l^H] = \text{tr}[(\mathbf{A}_l^H \mathbf{A}_l)^2]$ yields the desired result. ■

Corollary 3. With MRC at the BS consisting of a SC ULA, the expected uplink SINR of terminal l with LoS i.e., correlated Ricean fading, with equal correlation matrices for each terminal can be approximated as

$$\mathbb{E}[\text{SINR}_l^{C3}] \approx \frac{\rho \beta_l \delta_l}{\chi_l + \rho \sum_{k=1, k \neq l}^L \beta_k \varphi'_{l,k}}, \quad (21)$$

where

$$\varphi'_{l,k} = (\eta'_l)^2 (\eta'_k)^2 \text{tr}[(\mathbf{A}_l \mathbf{A}_l^H)^2] + (\eta'_l)^2 (\bar{\eta}_k)^2 \text{tr}[\bar{\mathbf{h}}_k^H \mathbf{A}_k \mathbf{A}_l^H \bar{\mathbf{h}}_k] + (\bar{\eta}_l)^2 (\eta'_k)^2 \text{tr}[\bar{\mathbf{h}}_l^H \mathbf{A}_l \mathbf{A}_k^H \bar{\mathbf{h}}_l] + (\bar{\eta}_l)^2 (\bar{\eta}_k)^2 M^2. \quad (22)$$

Proof: Replacing $\text{tr}[\mathbf{A}_k \mathbf{A}_k^H \mathbf{A}_l \mathbf{A}_l^H]$ with $\text{tr}[(\mathbf{A}_l \mathbf{A}_l^H)^2]$ yields the desired expression in (21). We note that δ_l and χ_l are as defined in (11) and (13), respectively. ■

Remark 4. Corollaries 1 and 2 share a common trend in that both the numerators and denominators are governed by spatial correlation matrices in \mathbf{A}_l and \mathbf{A}_k , respectively. In the case where correlation matrices are fixed for each terminal, the trace in their respective denominators can be readily seen to translate from $\text{tr}[\mathbf{A}_k \mathbf{A}_k^H \mathbf{A}_l \mathbf{A}_l^H]$ to $\text{tr}[(\mathbf{A}_l^H \mathbf{A}_l)^2]$.

In the subsequent section, we analyze the convergence of the expected per-terminal SINR and ergodic spectral efficiency with MRC, as the number of receive antennas, M , grows without bound with a fixed number of user terminals, L .

V. LIMITING EXPECTED PER-TERMINAL SINR AND ERGODIC SUM SPECTRAL EFFICIENCY ANALYSIS

Theorem 1 presents an expected uplink SINR approximation for terminal l which is suitable for any system size, as well as any operating SNR, LoS level, spatial correlation level and physical array spacing. We now examine the asymptotic behavior of (17), as $M \rightarrow \infty$, with a fixed (finite) L . Dividing through by M^2 throughout, we observe the limit as

$$\overline{\mathbb{E}[\text{SINR}_l]} = \lim_{M \rightarrow \infty} \left\{ \frac{\rho \beta_l (\delta_l / M^2)}{(\chi_l / M^2) + \rho \sum_{k=1, k \neq l}^L \beta_k (\varphi_{l,k} / M^2)} \right\}. \quad (23)$$

Referring to the numerator of (23), two terms in

$$\delta_l^1 = (\eta'_l)^4 (\text{tr}[(\mathbf{A}_l^H \mathbf{A}_l)^2] / M^2), \quad (24)$$

and

$$\delta_l^2 = 2 (\eta'_l)^2 (\bar{\eta}_l)^2 (\bar{\mathbf{h}}_l^H \mathbf{A}_l \mathbf{A}_l^H \bar{\mathbf{h}}_l / M^2), \quad (25)$$

do not vanish from δ_l as M grows without bound, whilst the denominator of (23) has four terms, these are

$$\varphi_{l,k}^1 = (\eta'_l)^2 (\eta'_k)^2 (\text{tr}[\mathbf{A}_k \mathbf{A}_k^H \mathbf{A}_l \mathbf{A}_l^H] / M^2), \quad (26)$$

$$\varphi_{l,k}^2 = (\eta'_l)^2 (\bar{\eta}_k)^2 (\text{tr}[\bar{\mathbf{h}}_k^H \mathbf{A}_k \mathbf{A}_l^H \bar{\mathbf{h}}_k] / M^2), \quad (27)$$

$$\varphi_{l,k}^3 = (\bar{\eta}_l)^2 (\eta'_k)^2 (\text{tr}[\bar{\mathbf{h}}_l^H \mathbf{A}_l \mathbf{A}_k^H \bar{\mathbf{h}}_l] / M^2), \quad (28)$$

and

$$\varphi_{l,k}^4 = (\bar{\eta}_l)^2 (\bar{\eta}_k)^2 (\bar{\mathbf{h}}_l^H \bar{\mathbf{h}}_k \bar{\mathbf{h}}_k^H \bar{\mathbf{h}}_l / M^2), \quad (29)$$

which do not vanish from $\varphi_{l,k}$ as $M \rightarrow \infty$.

In the sequel, Lemmas 4, 5 and 6 derive the limiting value of (24)-(29), respectively.

Lemma 4. $\lim_{M \rightarrow \infty} \varphi_{l,k}^4$ is given by

$$\begin{aligned} \bar{\varphi}_{l,k}^4 &= (\bar{\eta}_l)^2 (\bar{\eta}_k)^2 \lim_{M \rightarrow \infty} \left\{ \left| \frac{\bar{\mathbf{h}}_l^H \bar{\mathbf{h}}_k}{M} \right|^2 \right\} \\ &= (\bar{\eta}_l)^2 (\bar{\eta}_k)^2 \vartheta(\bar{\phi}_l, \bar{\phi}_k)^2, \end{aligned} \quad (30)$$

where $\vartheta(\bar{\phi}_l, \bar{\phi}_k) = |\text{sinc}(\pi d_0 (\sin(\bar{\phi}_l) - \sin(\bar{\phi}_k)) / \lambda)|$, where $\text{sinc}(\cdot)$ denotes the sinc function.

Proof: We begin by defining

$$\begin{aligned} \vartheta(\bar{\phi}_l, \bar{\phi}_k) &= \lim_{M \rightarrow \infty} \left\{ \left| \frac{\bar{\mathbf{h}}_l^H \bar{\mathbf{h}}_k}{M} \right| \right\} \\ &= \lim_{M \rightarrow \infty} \left\{ \left| \frac{1}{M} \sum_{c=0}^{M-1} e^{j2\pi \frac{d_0}{\lambda} \frac{a_0}{M-1} (\sin(\bar{\phi}_l) - \sin(\bar{\phi}_k))} \right| \right\} \\ &= \left| \int_0^1 e^{j2\pi \frac{d_0}{\lambda} (\sin(\bar{\phi}_l) - \sin(\bar{\phi}_k)) f} df \right| \\ &= |\text{sinc}(\pi d_0 (\sin(\bar{\phi}_l) - \sin(\bar{\phi}_k)) / \lambda)|, \end{aligned} \quad (31)$$

yielding the desired result. ■

Remark 5. The expression in (30) is another closed-form solution and can be readily seen to be dependent on the respective LoS angles unique to terminals l and k .

Lemma 5. $\lim_{M \rightarrow \infty} \varphi_{l,k}^3$ is given by

$$\begin{aligned} \bar{\varphi}_{l,k}^3 &= (\bar{\eta}_l)^2 (\eta'_k)^2 \lim_{M \rightarrow \infty} \left\{ \frac{\text{tr}[\bar{\mathbf{h}}_l^H \mathbf{A}_k \mathbf{A}_k^H \bar{\mathbf{h}}_l]}{M^2} \right\} \\ &= (\bar{\eta}_l)^2 (\eta'_k)^2 \sum_{r=1}^P \vartheta(\bar{\phi}_l, \phi_{k,r})^2. \end{aligned} \quad (32)$$

Proof: Using similar methodology as in the proof of Lemma 4, we recognize that

$$\frac{1}{M^2} \text{tr} [\mathbf{h}_l^H \mathbf{A}_k \mathbf{A}_k^H \mathbf{h}_l] = \frac{1}{M^2} \sum_{r=1}^P |\bar{\mathbf{h}}_l^H \mathbf{A}_k|^2. \quad (33)$$

Substituting the specular and diffuse angles, $\bar{\phi}_l$ and $\phi_{k,r}$ with $r \in \{1, \dots, P\}$, corresponding to $\bar{\mathbf{h}}_l$ and \mathbf{A}_k , yields (33). ■

Remark 6. We note that as $\varphi_{l,k}^2$ and δ_l^2 have a similar structure to $\varphi_{l,k}^3$, the limiting values of $\varphi_{l,k}^2$ and δ_l^2 in $\bar{\varphi}_{l,k}^2$ and $\bar{\delta}_l^2$ have the same form as (32), except the angles in $\vartheta(\cdot)$ are replaced with $\bar{\phi}_k, \phi_{l,r}$ for $\bar{\varphi}_{l,k}^2$ and $\bar{\phi}_l, \phi_{l,r}$ for $\bar{\delta}_l^2$, respectively. We further note that both $\bar{\varphi}_{l,k}^2$ and $\bar{\delta}_l^2$ will need to have the necessary scaling of $(\eta'_l)^2 (\bar{\eta}_k)^2$ and $2(\eta'_l)^2 (\bar{\eta}_l)^2$ as shown in (27) and (25).

Lemma 6. $\lim_{M \rightarrow \infty} \varphi_{l,k}^1$ is given by

$$\begin{aligned} \bar{\varphi}_{l,k}^1 &= (\eta'_l)^2 (\eta'_k)^2 \lim_{M \rightarrow \infty} \left\{ \frac{\text{tr} [\mathbf{A}_k \mathbf{A}_k^H \mathbf{A}_l \mathbf{A}_l^H]}{M^2} \right\} \\ &= (\eta'_l)^2 (\eta'_k)^2 \sum_{r=1}^P \sum_{t=1}^P \vartheta(\phi_{k,r}, \phi_{l,t})^2. \end{aligned} \quad (34)$$

Proof: Manipulating the trace in (34) allows us to state

$$\begin{aligned} \frac{1}{M^2} \{\text{tr} [\mathbf{A}_k \mathbf{A}_k^H \mathbf{A}_l \mathbf{A}_l^H]\} &= \frac{1}{M^2} \{\text{tr} [\mathbf{A}_k^H \mathbf{A}_l \mathbf{A}_l^H \mathbf{A}_k]\} \\ &= \frac{1}{M^2} \sum_{r=1}^P \sum_{t=1}^P |\mathbf{a}^H(\phi_{k,r}) \mathbf{a}(\phi_{l,t})|^2. \end{aligned} \quad (35)$$

Substituting the respective angles and performing some routine algebra yields the desired result. ■

Remark 7. We note that as δ_l^1 has a similar form to $\varphi_{l,k}^1$. Using the same methodology as in Lemma 6, we can obtain $\bar{\delta}_l^1$, the limiting value of δ_l^1 , where the angles in $\vartheta(\cdot)$ are replaced by $\phi_{l,r}, \phi_{l,t}$ with $(\eta'_l)^4$ providing the required scaling.

Theorem 2. The limiting uplink SINR for terminal l with MRC and a SC ULA at the BS can be written as

$$\mathbb{E}[\text{SINR}_l] = \frac{\rho \beta_l (\bar{\delta}_l^1 + \bar{\delta}_l^2)}{\rho \sum_{\substack{k=1 \\ k \neq l}}^L \beta_k (\bar{\varphi}_{l,k}^1 + \bar{\varphi}_{l,k}^2 + \bar{\varphi}_{l,k}^3 + \bar{\varphi}_{l,k}^4)}. \quad (36)$$

Proof: Using the results from Lemmas 4, 5, 6 and keeping in mind Remarks 6 and 7 yields the desired expression. ■

As such the limiting ergodic sum spectral efficiency is given by

$$\mathbb{E}[\mathbf{R}_{\text{sum}}] = \sum_{l=1}^L \log_2 \left(1 + \mathbb{E}[\text{SINR}_l] \right). \quad (37)$$

In the following section, we demonstrate the accuracy of the analysis presented in Sections III, IV and V, respectively.

VI. NUMERICAL RESULTS

Unless otherwise specified, the parameters used in the numerical results are specified in Table I for an UMi scenario. The parameters for microwave and mmWave frequencies were obtained from [17] and [10], respectively. A circular cell of radius 100 m is considered with an exclusion radius of $r_0 = 10$ m. We assume a uniform distribution of terminals in the cell area and consider 10^4 Monte-Carlo realizations

for each result. The parameter ϱ is chosen such that the fifth percentile value of the instantaneous per-terminal SINR is 0 dB at SNR (ρ) = 0 dB for the system dimensions of $M = 256$ and $L = 32$.

Parameter	Value	
	Microwave	mmWave
Carrier frequency [GHz]	2	28
LoS attenuation exponent [α]	2.2	2
NLoS attenuation exponent	3.67	2.92
LoS shadow fading standard deviation [σ_{sh}]	3	5.8
NLoS shadow fading standard deviation	4	8.7
K -Factor mean [dB]	9	12 [20]
K -Factor standard deviation [dB]	5	3 [20]

TABLE I
SYSTEM PARAMETERS

Based on the link distance, r_l , we employ a probability based approach in determining whether the terminal experiences LoS or NLoS conditions on the uplink to the BS. For the microwave case, the probability of terminal l experiencing LoS is governed by $P_{\text{LoS}}(r_l) = (\min(18/r_l, 1) (1 - e^{-r_l/36})) + e^{-r_l/36}$. Naturally, the probability of the terminal experiencing NLoS is then determined by $P_{\text{NLoS}} = 1 - P_{\text{LoS}}$. Equivalently, for the mmWave case [10], $P_{\text{LoS}}(r_l) = (1 - P_{\text{out}}(r_l)) e^{-\omega_{\text{LoS}} r_l}$, where $1/\omega_{\text{LoS}} = 67.1$ meters and P_{out} is the outage probability, occurring when the attenuation in either the LoS or NLoS states is sufficiently large. For simplicity, we set $P_{\text{out}} = 0$ when determining the LoS and NLoS probabilities. Upon determining the link state of each terminal, we select the corresponding link parameters to model the large-scale propagation effects of geometric attenuation and shadow-fading, as specified in Table I. We assign a unique K -factor, K_l , for the l -th user terminal from a log-normal distribution with the mean and standard deviation specified in Table I. We refer to this as $K_l \sim \ln(\text{mean}, \text{standard deviation})$.

First, the accuracy of the proposed expected per-terminal SINR in (17) is examined. Fig. 1 illustrates the expected SINR of a given terminal as a function of ρ (SNR) for a system with $M = 256$ and $L = 32$, $P = 50$ and $d_0 = 8\lambda$. In addition to the microwave and mmWave cases, we consider the correlated Rayleigh fading case for comparison purposes. We also consider the case where each terminal is assigned a fixed K -factor of 5 dB. Three trends can be observed: Firstly, transitioning from large to small angular spread ($\Delta \sim u[-\frac{\pi}{2}, \frac{\pi}{2}]$ to $\Delta \sim u[-\frac{\pi}{16}, \frac{\pi}{16}]$) tends to significantly reduce the expected SINR for all cases. This is despite the fact that the ULA contains very large numbers of antenna elements at the BS, and is due to the reduction in the spatial diversity (rank) of the channel, allowing the BS array to only see a very narrow spread of incoming power. Secondly, increasing the mean of K has an adverse effect on the expected SINR. This is because a stronger specular component in the channel tends to reduce the multipath diversity and in-turn reduces its overall rank. Equivalently, this can be interpreted as an increase in the level of inter-terminal interference leading to a lower expected per-terminal SINR. Third, our proposed approximations are seen to remain extremely tight for the entire SNR range for all

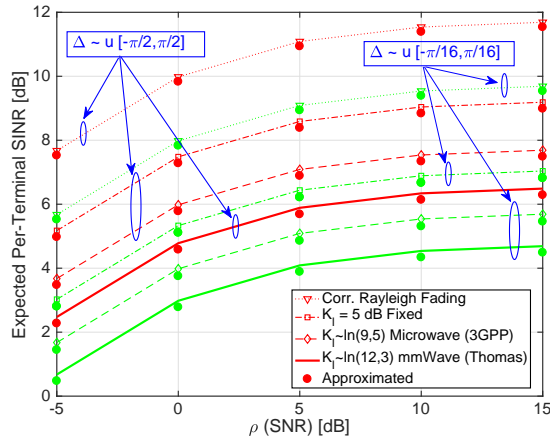


Fig. 1. Expected per-terminal SINR vs. ρ (SNR) with $M = 256, L = 32, P = 50, d_0 = 8\lambda$.

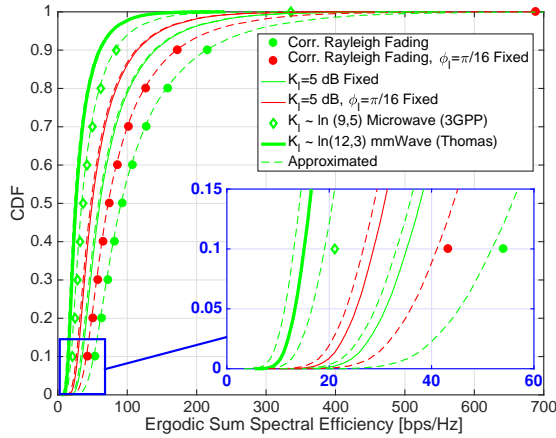


Fig. 2. Ergodic sum spectral efficiency CDF with $M = 256, L = 32, \rho$ (SNR) = 10 dB, $P = 50, d_0 = 8\lambda$ and $\Delta \sim u[-\frac{\pi}{16}, \frac{\pi}{16}]$ (unless specified in the figure).

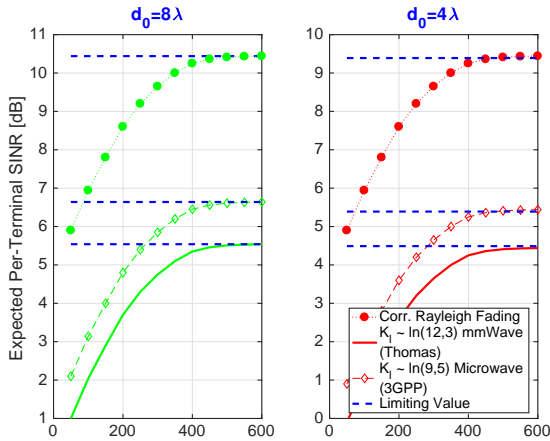


Fig. 3. Expected Per-Terminal SINR vs. M with $L = 32$ at ρ (SNR) = 10 dB, $P = 50, \Delta \sim u[-\frac{\pi}{16}, \frac{\pi}{16}]$.

cases. The analytical expressions are also seen to remain tight for the special case presented in (19), where each terminal undergoes Rayleigh fading with unequal correlation matrices. Furthermore, the expected SINR in each case is seen to saturate with growing SNR, due to the inability of the MRC to mitigate inter-terminal interference.

Considering the special cases in (20) and (21), we now

examine the influence of LoS, as well as equal and unequal correlation matrices on the ergodic sum spectral efficiency, as shown in Fig. 2. Using the same propagation parameters from Fig. 1, (listed in the figure caption) at ρ (SNR) = 10 dB, we compare the cumulative distribution functions (CDFs) of the derived ergodic sum spectral efficiency approximation in (18) with its simulated counterparts. We note that the CDF is obtained by averaging over the fast-fading in the channel with each value representing the variations in the link gains and K -factors. We notice that irrespective of the underlying propagation characteristics (Rayleigh or Ricean fading), unequal correlation matrices results in a higher ergodic sum spectral efficiency of the system allowing the ULA to leverage a larger amount of spatial diversity. Furthermore, we again observe that a stronger specular component tends to decrease the ergodic sum spectral efficiency. The derived approximations are robust to the presence of equal and unequal correlation matrices, as well as changes in the level of LoS. We also evaluate the accuracy of the limiting expected SINR expression derived in (36), with growing numbers of BS antennas and a fixed number of terminals in the system at $L = 32$. Three trends can be observed: After recognizing that increasing M increases the expected SINR, for each case the expected SINR slowly saturates with growing M and approaches its limiting value at approximately 500 antenna elements for each case, respectively. This is a result of channels from multiple terminals becoming asymptotically orthogonal. Secondly, decreasing the physical size of the array further reduces the inter-element spacing translating into a reduction in the expected SINR for all cases respectively. Finally, we can observe that each case converges to the derived limiting value.

VII. CONCLUSION

In this paper, we investigated the uplink performance of large MU-MIMO systems under spatially correlated Ricean fading, with ULAs at the BS employed in a fixed physical space. Closed-form approximations to the expected per-terminal SINR and ergodic sum spectral efficiency are derived with MRC processing at the BS. In the limit of a large number of BS antennas, asymptotic expressions for the expected per-terminal SINR and ergodic sum spectral efficiency were derived. Our numerical results show that with constraints on the physical size of the ULA, the expected SINR saturated with increasing SNR and BS antenna numbers. The analysis accommodates to changes in system dimensions, operating SNR, LoS levels, spatial correlation levels and variation in fixed physical spacings. Unequal correlation matrices to each terminal resulted in a performance increase, whilst LoS had an adverse impact on system performance.

APPENDIX A

PROOF OF LEMMA 1

We begin by recognizing $\delta_l = \mathbb{E}[\|g_l\|^4] = \mathbb{E}[(\|g_l\|^2)^2]$. Substituting the definition of g_l and denoting $v_l = \eta_l^H A_l h_l$ and $q_l = \bar{\eta}_l^H \bar{h}_l$ allows us to state

$$\delta_l = \mathbb{E}[(\|g_l\|^2)^2] = \mathbb{E}[(v_l^H v_l + v_l^H q_l + q_l^H v_l + q_l^H q_l)^2]. \quad (38)$$

Expanding (38) and simplifying allows us to state

$$\delta_l = \mathbb{E} \left[(||\mathbf{g}_l||^2)^2 \right] = \mathbb{E}[(\mathbf{v}_l^H \mathbf{v}_l)^2] + \mathbb{E}[2(\mathbf{v}_l^H \mathbf{v}_l)(\mathbf{q}_l^H \mathbf{q}_l)] + \mathbb{E}[\mathbf{v}_l^H \mathbf{q}_l \mathbf{q}_l^H \mathbf{v}_l] + \mathbb{E}[\mathbf{q}_l^H \mathbf{v}_l \mathbf{v}_l^H \mathbf{q}_l] + \mathbb{E}[(\mathbf{q}_l^H \mathbf{q}_l)^2]. \quad (39)$$

Performing the expectation over \mathbf{v}_l in the last four terms of (39) and simplifying yields

$$\delta_l = \mathbb{E} \left[(||\mathbf{g}_l||^2)^2 \right] = \mathbb{E}[(\mathbf{v}_l^H \mathbf{v}_l)^2] + 2(\mathbf{q}_l^H \mathbf{q}_l) PM(\eta'_l)^2 + 2(\eta'_l)^2 \mathbf{q}_l^H \mathbf{A}_l \mathbf{A}_l^H \mathbf{q}_l + (\mathbf{q}_l^H \mathbf{q}_l \mathbf{q}_l^H \mathbf{q}_l). \quad (40)$$

After recognizing that $\mathbb{E}[(\mathbf{v}_l^H \mathbf{v}_l)^2] = \mathbb{E}[\mathbf{v}_l^H \mathbf{v}_l \mathbf{v}_l^H \mathbf{v}_l]$, substituting the definition of \mathbf{v}_l and extracting the relevant constants allows us to write

$$\mathbb{E}[(\mathbf{v}_l^H \mathbf{v}_l)^2] = (\eta'_l)^4 \mathbb{E}[(\mathbf{h}_l^H \boldsymbol{\Theta} \mathbf{h}_l)^2], \quad (41)$$

where $\boldsymbol{\Theta} = \boldsymbol{\Psi}^H \boldsymbol{\Gamma} \boldsymbol{\Psi}$ is an eigenvalue decomposition of $\mathbf{A}_l^H \mathbf{A}_l$. As a result,

$$\begin{aligned} \mathbb{E}[(\mathbf{v}_l^H \mathbf{v}_l)^2] &= (\eta'_l)^4 \mathbb{E}[(\mathbf{h}_l^H \boldsymbol{\Gamma} \mathbf{h}_l)^2] \\ &= (\eta'_l)^4 \mathbb{E} \left[\left(\sum_{p=1}^P [\boldsymbol{\Gamma}]_{p,p} |\mathbf{h}_{l;p}|^2 \right)^2 \right], \end{aligned} \quad (42)$$

where $\mathbf{h}_{l;p}$ denotes the p -th element of \mathbf{h}_l . Performing the expectation with respect to \mathbf{h}_l and further simplifying yields

$$\mathbb{E}[(\mathbf{v}_l^H \mathbf{v}_l)^2] = (\eta'_l)^4 \left\{ (\text{tr}[\boldsymbol{\Theta}])^2 + \text{tr}[\boldsymbol{\Theta}^2] \right\}. \quad (43)$$

This allows us to write

$$\mathbb{E}[(\mathbf{v}_l^H \mathbf{v}_l)^2] = (\eta'_l)^4 \left\{ (\text{tr}[\mathbf{A}_l^H \mathbf{A}_l])^2 + \text{tr}[\mathbf{A}_l^H \mathbf{A}_l \mathbf{A}_l^H \mathbf{A}_l] \right\}. \quad (44)$$

Recognizing that $\text{tr}[\mathbf{A}_l^H \mathbf{A}_l] = PM$ allows us to state

$$\mathbb{E}[(\mathbf{v}_l^H \mathbf{v}_l)^2] = (\eta'_l)^4 \left\{ P^2 M^2 + \text{tr}[(\mathbf{A}_l^H \mathbf{A}_l)^2] \right\}. \quad (45)$$

Substituting the definition of \mathbf{q}_l back, recognizing that $\mathbb{E}[\bar{\mathbf{h}}_l^H \mathbf{h}_l] = M$, combining (45) with the remaining terms in (40) and extracting the relevant constants results in the desired expression.

APPENDIX B PROOF OF LEMMA 2

Applying the definition of \mathbf{g}_l and \mathbf{g}_k into $\mathbb{E}[|\mathbf{g}_l^H \mathbf{g}_k|^2]$ and denoting $\mathbf{v}_l = \eta'_l \mathbf{A}_l \mathbf{h}_l$ and $\mathbf{q}_l = \bar{\eta}_l \bar{\mathbf{h}}_l$ yields

$$\varphi_l = \mathbb{E}[|\mathbf{g}_l^H \mathbf{g}_k|^2] = \mathbb{E}[|(\mathbf{v}_l^H + \mathbf{q}_l^H)(\mathbf{v}_k + \mathbf{q}_k)|^2]. \quad (46)$$

Expanding and simplifying (46) allows us to state

$$\begin{aligned} \varphi_l &= \mathbb{E}[|\mathbf{g}_l^H \mathbf{g}_k|^2] = \mathbb{E}[(\mathbf{v}_l^H \mathbf{v}_k + \mathbf{v}_l^H \mathbf{q}_k + \mathbf{q}_l^H \mathbf{v}_k + \mathbf{q}_l^H \mathbf{q}_k) \\ &\quad (\mathbf{v}_k^H \mathbf{v}_l + \mathbf{q}_k^H \mathbf{v}_l + \mathbf{v}_k^H \mathbf{q}_l + \mathbf{q}_k^H \mathbf{q}_l)]. \end{aligned} \quad (47)$$

Further expanding and simplifying yields

$$\begin{aligned} \varphi_l &= \mathbb{E}[|\mathbf{g}_l^H \mathbf{g}_k|^2] = \mathbb{E}[\mathbf{v}_l^H \mathbf{v}_k \mathbf{v}_k^H \mathbf{v}_l] + \mathbb{E}[\mathbf{v}_l^H \mathbf{q}_k \mathbf{q}_k^H \mathbf{v}_l] + \\ &\quad \mathbb{E}[\mathbf{q}_l^H \mathbf{v}_k \mathbf{v}_k^H \mathbf{q}_l] + \mathbb{E}[\mathbf{q}_l^H \mathbf{q}_k \mathbf{q}_k^H \mathbf{q}_l]. \end{aligned} \quad (48)$$

Invoking the independence between \mathbf{v}_l and \mathbf{v}_k , recognizing that $\mathbb{E}[\mathbf{v}_l \mathbf{v}_l^H] = (\eta'_l)^2 \text{tr}[\mathbf{A}_l^H \mathbf{A}_l]$, upon substituting back the definitions of \mathbf{v}_k and \mathbf{q}_k and extracting the relevant constants, we can state

$$\begin{aligned} \varphi_l &= \mathbb{E}[|\mathbf{g}_l^H \mathbf{g}_k|^2] = (\eta'_l)^2 (\eta'_k)^2 \mathbb{E}[\mathbf{h}_l^H \mathbf{A}_l^H \mathbf{A}_k \mathbf{A}_k^H \mathbf{h}_l] + (\eta'_l)^2 (\bar{\eta}_k)^2 [\bar{\mathbf{h}}_k^H \mathbf{A}_l \\ &\quad \mathbf{A}_l^H \bar{\mathbf{h}}_k] + (\bar{\eta}_l)^2 (\eta'_k)^2 [\bar{\mathbf{h}}_l^H \mathbf{A}_k \mathbf{A}_k^H \bar{\mathbf{h}}_l] + (\bar{\eta}_l)^2 (\bar{\eta}_k)^2 [|\bar{\mathbf{h}}_l^H \bar{\mathbf{h}}_k|^2]. \end{aligned} \quad (49)$$

Taking the trace and simplifying yields the result in (12).

ACKNOWLEDGMENT

The authors would like to thank Prof. Andreas F. Molisch at the University of Southern California for the insightful discussions during the course of this work.

REFERENCES

- [1] F. Rusek, D. Persson, B. Lau, E. G. Larsson, T. L. Marzetta, O. Edfors, and F. Tufvesson, "Scaling up MIMO: Opportunities and challenges with very large arrays", *IEEE Signal Process. Mag.*, vol. 30, no. 1, pp. 40-60, Nov. 2013.
- [2] E. G. Larsson, O. Edfors, F. Tufvesson, and T. L. Marzetta, "Massive MIMO for next generation wireless systems", *IEEE Commun. Mag.*, vol. 52, no. 2, pp. 186-195, Feb. 2014.
- [3] C. Masouros, M. Sellathurai, and T. Ratnarajah, "Large-scale MIMO transmitters in fixed physical spaces: The effect of transmit correlation and mutual coupling", *IEEE Trans. Commun.*, vol. 61, no. 7, pp. 2794-2804, Jul. 2013.
- [4] C. Masouros and M. Matthaiou, "Space-constrained massive MIMO: Hitting the wall of favorable propagation", *IEEE Commun. Lett.*, vol. 19, no. 5, pp. 771-774, May 2015.
- [5] H. Q. Ngo, E. G. Larsson, and T. L. Marzetta, "The multicell multiuser MIMO uplink with very large antenna arrays and a finite-dimensional channel", *IEEE Trans. Commun.*, vol. 6, no. 61, pp. 2350-2361, Jun. 2013.
- [6] A. Garcia-Rodriguez and C. Masouros, "Exploiting the increasing correlation of space constrained massive MIMO for CSI relaxation", *IEEE Trans. Commun.*, vol. 4, no. 64, pp. 1572-1587, Apr. 2016.
- [7] J. Zhang, L. Dai, M. Matthaiou, C. Masouros, and S. Jin, "On the spectral efficiency of space-constrained massive MIMO with linear receivers", in *Proc. of IEEE Int. Conf. on Commun. (ICC)*, pp. 1-6, May 2016.
- [8] S. Biswas, C. Masouros, and T. Ratnarajah, "Performance analysis of large multi-user MIMO systems with space-constrained 2D antenna arrays", *IEEE Trans. Wireless Commun.*, vol. 15, no. 5, pp. 3492-3505, May 2016.
- [9] X. Ge, R. Zi, H. Wang, J. Zhang, and M. Jo, "Multi-user massive MIMO communication systems based on irregular antenna arrays", *IEEE Trans. Wireless Commun.*, vol. 15, no. 8, pp. 5287-5301, Aug. 2016.
- [10] M. R. Akdeniz, Y. Liu, M. K. Samimi, S. Sun, S. Rangan, T. S. Rappaport, and E. Erkip, "Millimeter wave channel modeling and cellular capacity evaluation", *IEEE J. Sel. Areas Commun.*, vol. 32, no. 6, pp. 1164-1179, Jun. 2014.
- [11] S. Sun, T. S. Rappaport, R. W. Heath Jr., A. R. Nix, and S. Rangan, "MIMO for millimeter-wave wireless communications: Beamforming, spatial multiplexing, or both?", *IEEE Commun. Mag.*, vol. 52, no. 12, pp. 110-121, Dec. 2014.
- [12] H. Tataria, P. J. Smith, L. J. Greenstein, P. A. Dmochowski, and M. Shafi, "Performance and analysis of downlink multiuser MIMO systems with regularized zero-forcing precoding in Ricean fading channels", in *Proc. of IEEE Int. Conf. on Commun. (ICC)*, pp. 1185-1192, May 2016.
- [13] H. Tataria, P. J. Smith, L. J. Greenstein, and P. A. Dmochowski, "Zero-forcing precoding performance in multiuser MIMO systems with heterogeneous Ricean fading", *IEEE Wireless Commun. Lett.*, vol. 6, no. 1, pp. 74-77, Feb. 2017.
- [14] J. Nam, G. Caire, and J. Ha, "On the role of transmit correlation diversity in multiuser MIMO systems", *IEEE Trans. Info. Theory*, vol. 63, no. 1, pp. 336-354, Jan. 2017.
- [15] A. F. Molisch *Wireless Communications*, Wiley Press, 2011.
- [16] K. Warnick and M. Jensen, "Optimal noise matching for mutually coupled arrays", *IEEE Trans. Antennas Propag.*, vol. 55, no. 6, pp. 1726-1731, Jun. 2007.
- [17] 3GPP TR 36.873 v12.0.0, *Study on 3D channel models for LTE*, 3GPP, Jun. 2015.
- [18] Q. Zhang, S. Jin, K-K. Wong, H. Zhu, and M. Matthaiou, "Power scaling of uplink massive MIMO systems with arbitrary-rank channel means", *IEEE J. Sel. Topics Signal Process.*, vol. 8, no. 5, pp. 966-981, Nov. 2014.
- [19] D. Basnayaka, P. J. Smith, and P. A. Martin, "Performance analysis of macrodiversity MIMO systems with MMSE and ZF receivers in flat Rayleigh fading", *IEEE Trans. Wireless Commun.*, vol. 12, no. 5, pp. 2240-2251, May 2013.
- [20] T. Thomas, H. C. Nguyen, G. R. MacCartney, and T. S. Rappaport, "3D mmWave channel model proposal", in *Proc. IEEE Conf. on Veh. Technol. (VTC-Fall)*, pp. 1-6, Sep. 2014.